Impurity effects on electron–mode coupling in high-temperature superconductors

K. TERASHIMA[1], H. MATSUI[1], D. HASHIMOTO[1], T. SATO[1,2], T. TAKAHASHI[1,2]*, H. DING[3], T. YAMAMOTO[4] AND K. KADOWAKI[4]

[1]Department of Physics, Tohoku University, Sendai 980-8578, Japan
[2]CREST, Japan Science and Technology Agency (JST), Kawaguchi 332-0012, Japan
[3]Department of Physics, Boston College, Chestnut Hill, Massachusetts 02467, USA
[4]Institute of Materials Science, University of Tsukuba, Tsukuba 305-8573, Japan
*e-mail: t.takahashi@arpes.phys.tohoku.ac.jp

Published online: 25 December 2005; doi:10.1038/nphys200

Despite years of intensive research on copper oxide superconductors with high transition temperatures (T_c), the driving force of superconductivity has not yet been clarified. Angle-resolved photoemission spectroscopy (ARPES)[1–3] measurements have uncovered an important contribution of lattice vibrations (phonons) to superconductivity, sparking a fierce debate on the nature of the 'glue'—phonons or magnetic excitations—binding together the superconducting Cooper pairs[1–11]. However, it is difficult to distinguish these two pairing forces owing to their similar energy scales. Here, we propose a fresh approach to investigate the origin of many-body interactions in these superconductors: an impurity-substitution effect on the low-energy dynamics, which is a magnetic analogue of the isotope effect used for classical superconductors. Our ARPES results reveal that the impurity-induced changes in the electron self-energy show a good correspondence to those of magnetic excitations[12–18], indicating the importance of spin fluctuations to electron pairing in the high-T_c superconductors.

The interaction of electrons with bosonic excitations (phonons or spin excitations), which causes the pairing of electrons and leads to superconductivity, produces a small anomaly in the energy dispersion in the vicinity of the Fermi level (E_F); ref. 19. High-resolution ARPES has directly observed a small band anomaly, now known as a 'kink', in high-T_c cuprates. In order to clarify the origin of the kink and its relationship with the high-T_c superconductivity, the momentum, carrier concentration, temperature and CuO_2-layer-number dependences of the kink have been investigated intensively[1–3,5–11]. However, no consensus on the origin of the kink has yet been reached. The largest discrepancy is the assignment of the kink in the antinodal region around the $(\pi, 0)$ point in the Brillouin zone, where the dispersion kink is observed to be the strongest and the d-wave gap becomes maximum in the superconducting state. Three possible candidates, the magnetic mode[12–15], the B_{1g} phonon[20,21] and the longitudinal optical phonon[22], have been proposed. However, as all of these modes have similar energies of 40–70 meV, there are no convincing experimental clues to distinguish these apparently different possibilities. One effective approach to find the origin of the kink is to investigate the impurity effect using impurity atoms with different spin states but with similar atomic masses, because it is expected that even a small amount of such impurities will significantly affect the magnetic environment in the CuO_2 plane while not producing a marked change in the lattice vibration. This approach is regarded as an 'isotope' effect for magnetically mediated superconductors, analogous to the conventional isotope effect for phonon-mediated superconductors. Here, we report ultrahigh-resolution ARPES results on Zn-substituted and Ni-substituted samples of the Bi-based high-T_c cuprate superconductor $Bi_2Sr_2CaCu_2O_{8+\delta}$ (Bi2212) to find the origin of the kink and its relationship with the superconductivity, and to clarify how the interactions affecting the single-particle excitations are altered by impurity substitutions.

Figure 1 shows ARPES intensity plots as a function of wavevector and binding energy measured along the nodal and off-nodal cuts in the superconducting state (temperature $T = 40$ K) for pristine, Zn-substituted and Ni-substituted Bi2212. As is clearly seen in Fig. 1a, a characteristic dispersion kink appears in the pristine sample at approximately 50–80 meV in the nodal cut where the d-wave superconducting gap vanishes. This is in good agreement with the results of previous reports[1,7–9]. A similar kink is also observed in both Zn-substituted and Ni-substituted Bi2212 (Fig. 1g). We find that the kink in the off-nodal cut is relatively sensitive to the impurities as shown in Fig. 1d–f,h. As it is essential to measure spectra in the same cut in the Brillouin zone, we have verified that the cuts are in the same location for the three samples by precise Fermi-surface mapping. As shown in Fig. 1, the off-nodal kink is more prominent than the nodal kink in the superconducting state, and shows an 's-shaped' dispersion consistent with theoretical prediction[15]. On introducing Zn or Ni impurity, the off-nodal kink is weakened noticeably. We have confirmed that this impurity-induced change is reproducible and intrinsic by measuring many (>10) samples.

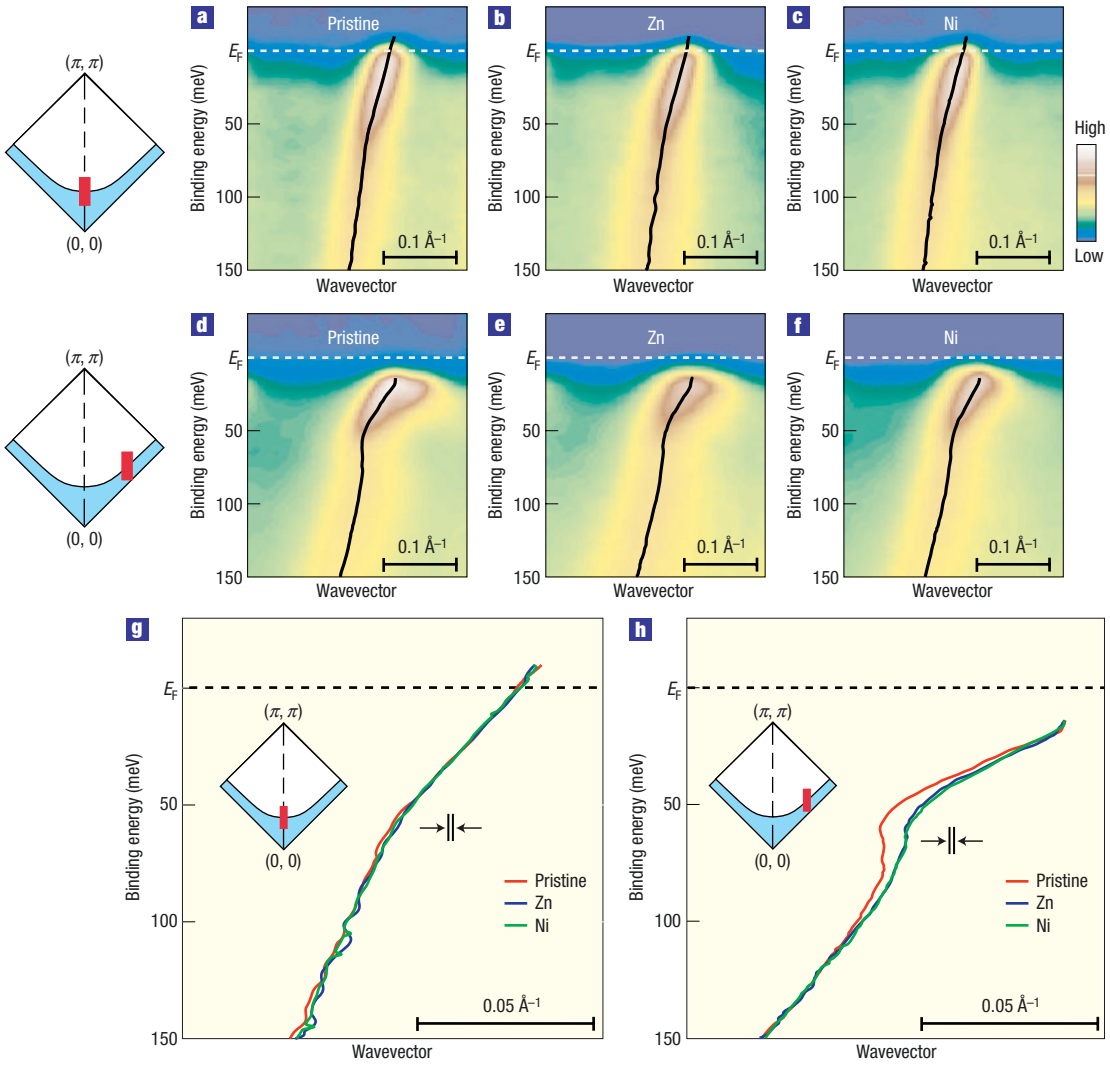

Figure 1 Impurity effects on energy dispersion near E_F in the superconducting state. ARPES intensity plots measured at 40 K along the nodal and off-nodal cuts for pristine, Zn-substituted and Ni-substituted Bi2212. The black curves show the peak positions of the momentum distribution curves (MDCs). The MDC is defined as the ARPES intensity as a function of momentum at a constant binding energy. **g** and **h**, Comparison of the three dispersions on an expanded scale. Arrows in **g** and **h** denote experimental uncertainties around 50 meV binding energy in determining the MDC peak position (0.002 Å^{-1}). The inset displays the Fermi surface and the measured locations of the nodal and off-nodal cuts (red bars) in the Brillouin zone. We do not use the ARPES data around the $(\pi, 0)$ region as the MDC analysis is hard to apply because of the flatness of the band dispersion around this momentum region.

The observed weakening of the kink cannot be simply attributed to the reduction in the size of the superconducting gap on impurity substitution (1–3 meV), which should cause a parallel shift in the energy dispersion towards E_F by 1–3 meV, inconsistent with the experimental result. Therefore, we think that the observed weakening of the kink in impurity-substituted Bi2212 reflects the impurity-induced change in the strength of the coupling between electrons and a certain low-energy excitation mode.

To see the change of the coupling strength more clearly, in Fig. 2a we plot the real part of the electron self-energy $\mathrm{Re}\Sigma(\omega)$, where ω is the energy relative to E_F, in the superconducting state estimated from the dispersions in Fig. 1h for pristine, Zn-substituted and Ni-substituted Bi2212. Following the procedure in the previous reports[7,9], we define $\mathrm{Re}\Sigma(\omega)$ as the energy difference between the observed energy dispersion and the linear dispersion line that passes two points at E_F and 250 meV in the experimental dispersion. The reason we use this criterion is that we can track the energy dispersion up to 250 meV with a reasonable count rate irrespective of sample angle (momentum) and impurity substitution. As seen in Fig. 2a, $\mathrm{Re}\Sigma(\omega)$ has a maximum ($\mathrm{Re}\Sigma(\omega)^{\mathrm{max}}$) of approximately 40 meV at a binding energy of 60 meV in pristine Bi2212, whereas on impurity substitution $\mathrm{Re}\Sigma(\omega)^{\mathrm{max}}$ is markedly reduced by approximately a half. This suggests that the coupling strength of electrons with the mode is substantially reduced in Zn-substituted and Ni-substituted Bi2212. Figure 2b shows the momentum dependence of $\mathrm{Re}\Sigma(\omega)^{\mathrm{max}}$ for pristine and Zn-substituted Bi2212. The $\mathrm{Re}\Sigma(\omega)^{\mathrm{max}}$ values of pristine and Zn-substituted Bi2212 are found to be almost the same around the nodal region (Fermi-surface angle $\phi = 35$–$45°$), whereas their difference is gradually enhanced on approaching the antinode ($\phi = 0°$) where the d-wave gap is maximal, because the $\mathrm{Re}\Sigma(\omega)^{\mathrm{max}}$ of pristine Bi2212 rapidly increases near the antinode. The enhancement of the difference in $\mathrm{Re}\Sigma(\omega)^{\mathrm{max}}$ around the antinodal region suggests that the impurity has greater effect on

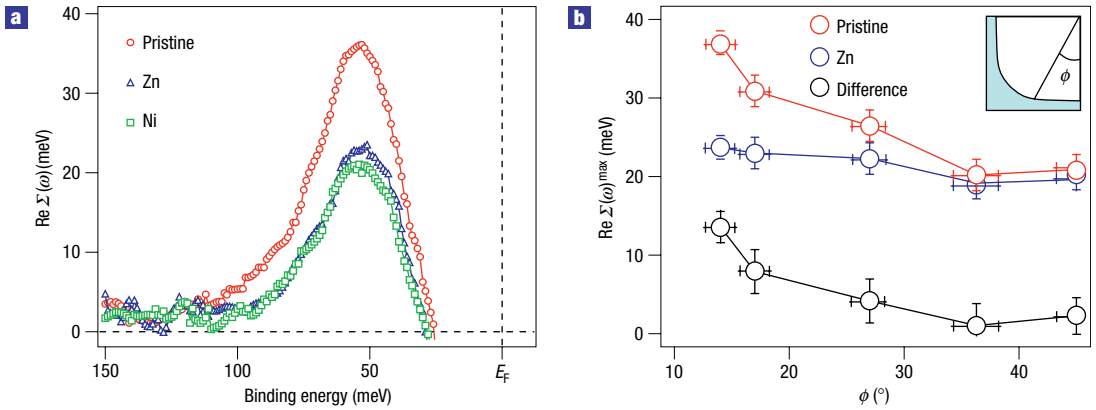

Figure 2 Energy and momentum dependence of the real part of the electron self-energy in the superconducting state. a, The real part of the self-energy, Re$\Sigma(\omega)$, for pristine, Zn-substituted and Ni-substituted Bi2212. **b**, Maximum values of Re$\Sigma(\omega)$ of pristine and Zn-substituted Bi2212 and the difference between them as a function of the Fermi-surface angle (ϕ) defined in the inset. Vertical and horizontal error bars denote the experimental uncertainty in determining the MDC peak position and the location on the Fermi surface, respectively, involving a combination of several physical parameters.

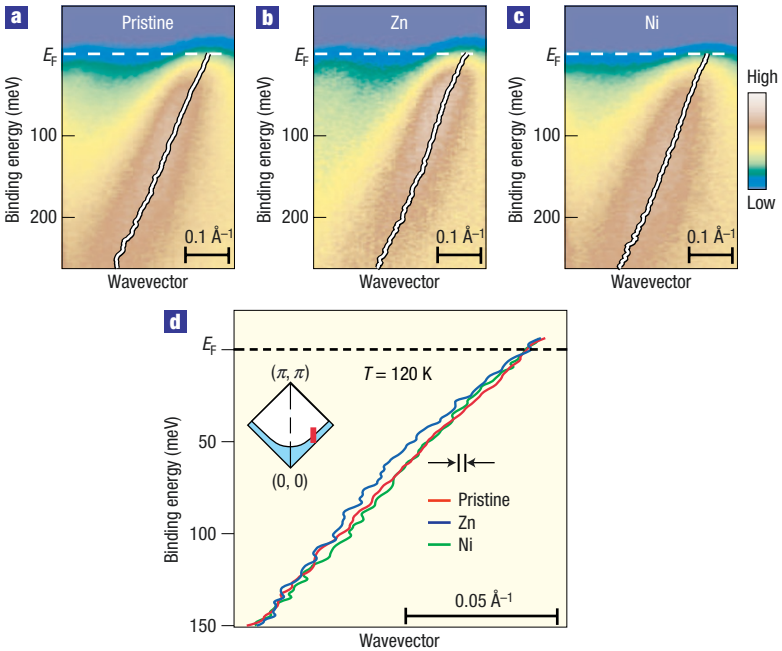

Figure 3 Impurity effects on energy dispersion near E_F above T_c. ARPES intensity plots measured along the off-nodal cut above T_c ($T = 120$ K) for **a**, pristine, **b**, Zn-substituted and **c**, Ni-substituted Bi2212. **d**, Comparison of the three dispersions on an expanded scale. Arrows denote the experimental uncertainty around 50 meV binding energy in determining the MDC peak position (0.003 Å^{-1}).

the kink in the antinodal region and the mode suppressed by the impurity strongly couples with electrons near $(\pi, 0)$.

Figure 3 shows ARPES intensity plots measured at the off-nodal cut above T_c ($T = 120$ K) for pristine, Zn-substituted and Ni-substituted Bi2212. We observed a leading-edge shift of 4 meV below E_F at 120 K for all the samples, indicative of the opening of a pseudogap. This pseudogap disappears at approximately 140 K. In Fig. 3, we find that the energy dispersion of pristine and Ni-substituted Bi2212 is almost straight, whereas that of Zn-substituted Bi2212 shows a small but detectable kink at approximately 50 meV, as clearly seen in Fig. 3d. This suggests that the coupling between electrons and the mode in the antinodal region, as seen in the superconducting state, survives even above T_c for Zn-substituted Bi2212 but not for pristine or Ni-substituted Bi2212. This observation strongly suggests that the electron–mode coupling in the antinodal region is very sensitive to the characteristics of the impurities.

The element sensitivity of the antinodal kink is further demonstrated in Fig. 4a, where the temperature dependence of Re$\Sigma(\omega)^{max}$ for the off-nodal cut in pristine, Zn-substituted and Ni-substituted Bi2212 is plotted. The Re$\Sigma(\omega)^{max}$ values of pristine and Ni-substituted Bi2212 gradually decrease with increasing temperature and almost vanish or saturate at their T_c. In contrast, the Re$\Sigma(\omega)^{max}$ value of Zn-substituted Bi2212 does not show

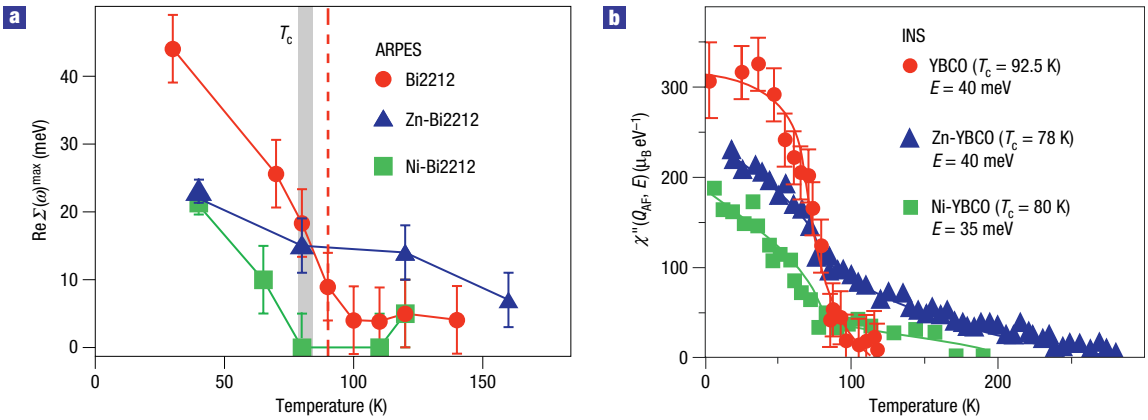

Figure 4 Comparison between electron self-energy from ARPES and spin susceptibility from INS experiments. a, Temperature dependence of Re$\Sigma(\omega)$ in pristine[9], Zn-substituted and Ni-substituted Bi2212 determined by ARPES. Error bars denote the experimental uncertainty in determining the MDC peak position, involving a combination of several physical parameters. **b**, Temperature dependence of the imaginary part of the spin susceptibility χ'' at $Q = Q_{AF} = (\pi, \pi)$, the antiferromagnetic wavevector, at the resonance energy measured by INS experiments for pristine, Zn-substituted and Ni-substituted YBCO[17,18] (μ_B is the Bohr magneton).

such saturation, but decreases monotonically even after passing T_c. This clear contrast suggests that the electron–mode coupling is affected differently by non-magnetic (Zn) and magnetic (Ni) impurities. Remarkably, a similar difference between magnetic and non-magnetic impurities has been reported in inelastic neutron scattering (INS) experiments[17,18]. Figure 4b shows the temperature dependence of the imaginary part of the spin susceptibility χ'' at the momentum transfer $Q = (\pi, \pi)$ at the resonance energy for pristine, Zn-substituted and Ni-substituted $YBa_2Cu_3O_{7-\delta}$ (YBCO)[17,18]. It is clear from the comparison between Fig. 4a and b that both physical properties (Re$\Sigma(\omega)^{max}$ and χ'') show similar temperature and impurity dependences, such as a decrease in magnitude on impurity substitution below T_c and a residual magnitude above T_c only for the Zn-substituted sample. This remarkable similarity between ARPES and INS demonstrates that the kink in the antinodal region is produced by the coupling between electrons and spin fluctuations. The good correspondence between Re$\Sigma(\omega)^{max}$ and χ'' above T_c for Zn-substituted samples suggests that the spin excitations near $Q = (\pi, \pi)$ play a dominant role in characterizing the energy dispersion in the antinodal region not only below T_c but also above T_c. The observed impurity-sensitive change in the energy dispersion in the antinodal region may not be explained by the B_{1g} or longitudinal optical phonon, because the substitution by only 1% impurities with almost the same mass number (Zn or Ni to Cu) is expected to hardly affect the lattice vibration, especially not for the oxygen phonons. The clear difference in the temperature dependences of non-magnetic (Zn) and magnetic (Ni) impurities is also difficult to explain in terms of electron–phonon coupling.

METHODS

High-quality single crystals of pristine, Zn-substituted and Ni-substituted $Bi_2Sr_2CaCu_2O_{8+\delta}$ were grown by the travelling-solvent floating-zone method. The content of Zn or Ni impurity was estimated to be 0.5–1.0% by electron-probe microanalysis together with the decrease in the T_c of substituted samples[23]. It is expected that Zn and Ni impurity atoms are substituted for Cu atoms in the CuO_2 planes as shown in scanning tunnelling microscopy experiments[24,25]. The T_c values are 91 K for pristine samples and 80–85 K for substituted samples. We have determined the hole concentration by precise Fermi-surface mapping, and the volumes (electrons per unit cell) are estimated to be 1.15, 1.16 and 1.15 for pristine, Zn-substituted and Ni-substituted Bi2212, respectively, which correspond to a 5% variation in hole concentration in the three samples. If we try to attribute the weakening of the kink and the decrease in T_c to the change in hole concentration in Zn-substituted and Ni-substituted Bi2212, the hole concentration should be changed by approximately 25% when we assume a dome-shaped relationship between T_c and hole concentration[26]. Therefore, we conclude that the observed weakening of the kink is not due to the doping effect.

High-resolution ARPES measurements were performed using GAMMADATA-SCIENTA SES-200 and SES-2002 spectrometers with a high-flux discharge lamp and a toroidal grating monochromator. We used the He Iα resonance line (21.218 eV) to excite photoelectrons. The energy and angular resolutions were set at 7–12 meV and 0.2°, respectively. The clean sample surface for ARPES measurement was obtained by *in situ* cleaving of crystals in an ultrahigh vacuum better than 7×10^{-11} torr. The Fermi level of the sample was referenced to that of a gold film evaporated on the sample substrate.

Received 7 August 2005; accepted 28 November 2005; published 25 December 2005.

References

1. Lanzara, A. *et al.* Evidence for ubiquitous strong electron-phonon coupling in high-temperature superconductors. *Nature* **412,** 510–514 (2001).
2. Gweon, G.-H. *et al.* An unusual isotope effect in a high-transition-temperature superconductor. *Nature* **430,** 187–190 (2004).
3. Cuk, T. *et al.* Coupling of the B_{1g} phonon to the antinodal electronic states of $Bi_2Sr_2Ca_{0.92}Y_{0.08}Cu_2O_{8+\delta}$. *Phys. Rev. Lett.* **93,** 117003 (2004).
4. Norman, M. R. *et al.* Unusual dispersion and line shape of the superconducting state spectra of $Bi_2Sr_2CaCu_2O_{8+\delta}$. *Phys. Rev. Lett.* **79,** 3506–3509 (1997).
5. Bogdanov, P. V. *et al.* Evidence for an energy scale for quasiparticle dispersion in $Bi_2Sr_2CaCu_2O_8$. *Phys. Rev. Lett.* **85,** 2581–2584 (2000).
6. Kaminski, A. *et al.* Renormalization of spectral line shape and dispersion below T_c in $Bi_2Sr_2CaCu_2O_{8+\delta}$. *Phys. Rev. Lett.* **86,** 1070–1073 (2001).
7. Johnson, P. D. *et al.* Doping and temperature dependence of the mass enhancement observed in the cuprate $Bi_2Sr_2CaCu_2O_{8+\delta}$. *Phys. Rev. Lett.* **87,** 177007 (2001).
8. Zhou, X. J. *et al.* Universal nodal Fermi velocity. *Nature* **423,** 398 (2003).
9. Sato, T. *et al.* Observation of band renormalization effects in hole-doped high-T_c superconductors. *Phys. Rev. Lett.* **91,** 157003 (2003).
10. Kim, T. K. *et al.* Doping dependence of the mass enhancement in $(Pb,Bi)_2Sr_2CaCu_2O_8$ at the antinodal point in the superconducting and normal states. *Phys. Rev. Lett.* **91,** 167002 (2003).
11. Gromko, A. D. *et al.* Mass-renormalized electronic excitations at $(\pi, 0)$ in the superconducting state of $Bi_2Sr_2CaCu_2O_{8+\delta}$. *Phys. Rev. B* **68,** 174520 (2003).
12. Rossat-Mignod, J. *et al.* Neutron scattering study of the $YBa_2Cu_3O_{6+x}$ system. *Physica C* **185–189,** 86–92 (1991).
13. Mook, H. A. *et al.* Polarized neutron determination of the magnetic excitations in $YBa_2Cu_3O_7$. *Phys. Rev. Lett.* **70,** 3490–3493 (1993).
14. Fong, H. F. *et al.* Neutron scattering from magnetic excitations in $Bi_2Sr_2CaCu_2O_{8+\delta}$. *Nature* **398,** 588–591 (1999).
15. Eschrig, M. & Norman, M. R. Effect of the magnetic resonance on the electronic spectra of high-T_c superconductors. *Phys. Rev. B* **67,** 144503 (2003).
16. Fong, H. F. *et al.* Effect of nonmagnetic impurities on the magnetic resonance peak in $YBa_2Cu_3O_7$. *Phys. Rev. Lett.* **82,** 1939–1942 (1999).
17. Sidis, Y. *et al.* Magnetic resonance peak and nonmagnetic impurities. Preprint at <http://arxiv.org/abs/cond-mat/0006265> (2000).
18. Sidis, Y. *et al.* Quantum impurities and the neutron resonance peak in $YBa_2Cu_3O_7$: Ni versus Zn. *Phys. Rev. Lett.* **84,** 5900–5903 (2000).

19. Scalapino, D. J. in *Superconductivity* (ed. Parks, R. D.) 449–560 (Marcel Dekker, New York, 1969).
20. Pyka, N. *et al.* Superconductivity-induced phonon softening in $YBa_2Cu_3O_7$ observed by inelastic neutron scattering. *Phys. Rev. Lett.* **70,** 1457–1460 (1993).
21. Devereaux, T. P., Cuk, T., Shen, Z.-X. & Nagaosa, N. Anisotropic electron-phonon interaction in the cuprates. *Phys. Rev. Lett.* **93,** 117004 (2004).
22. McQueeney, R. J. *et al.* Anomalous dispersion of LO phonons in $La_{1.85}Sr_{0.15}CuO_4$ at low temperatures. *Phys. Rev. Lett.* **82,** 628–631 (1999).
23. Maeda, A. *et al.* Substitution of 3d metals for Cu in $Bi_2(Sr_{0.6}Ca_{0.4})_3Cu_2O_y$. *Phys. Rev. B* **41,** 4112–4117 (1990).
24. Pan, S. H. *et al.* Imaging the effects of individual zinc impurity atoms on superconductivity in $Bi_2Sr_2CaCu_2O_{8+\delta}$. *Nature* **403,** 746–750 (2000).
25. Hudson, E. W. *et al.* Interplay of magnetism and high-T_c superconductivity at individual Ni impurity atoms in $Bi_2Sr_2CaCu_2O_{8+\delta}$. *Nature* **411,** 920–924 (2001).
26. Presland, M. R. *et al.* General trends in oxygen stoichiometry effects on T_c in Bi and Tl superconductors. *Physica C* **176,** 95–105 (1991).

Acknowledgements

This work was supported by grants from MEXT and JST-CREST of Japan and US NSF DMR-0353108. K.T. and H.M. thank JSPS for financial support.
Correspondence and requests for materials should be addressed to T.T.

Competing financial interests

The authors declare that they have no competing financial interests.